Effects of disorder on wave propagation in two-dimensional photonic crystals

A. A. Asatryan,[1] P. A. Robinson,[1] L. C. Botten,[2] R. C. McPhedran,[1] N. A. Nicorovici,[1] and C. Martijn de Sterke[1]
[1]*School of Physics, The University of Sydney, Sydney, New South Wales 2006, Australia*
[2]*School of Mathematical Sciences, University of Technology, Sydney, New South Wales 2007, Australia*
(Received 11 May 1999)

The electromagnetic transmittance of disordered two-dimensional photonic crystals composed of circular cylinders is investigated as a function of wavelength and polarization. At short wavelengths, the transmittance shows a band structure similar to that found in the optical absorption spectrum of amorphous semiconductors, with impurity states increasingly appearing on the long wavelength side of the band gaps as the degree of disorder is increased. In the long-wavelength limit, Anderson localization of waves is found, provided that the wavelength is not so large that the random photonic crystal can be viewed as homogeneous. The localization properties in this regime are studied and an analytic expression for the dependence of the localization length on wavelength is derived. In the limit of extremely long wavelengths, the system homogenizes and can be replaced by an equivalent one with uniform effective refractive index, whose form is derived for both polarizations. Analysis of the crossover between localization and homogenization is also presented.
[S1063-651X(99)18510-6]

PACS number(s): 41.20.Jb, 42.70.Qs, 73.20.−r

I. INTRODUCTION

Since the first suggestion by Yablonovitch [1] of the possibility of making materials which carry out the same function for photons as semiconductors do for electrons, the field of photonic crystals [the so-called photonic band-gap materials (PBG)] has been rapidly developing [2,3]. Now the study of photonic crystals is a subject of intense investigations [4]. Many possible applications of such materials have been proposed: optical switches [5], high-quality factor optical microcavities [6], and optimized antennas [7], to name but a few.

Though the number of papers that study the properties of photonic crystals is large [4], to our knowledge only Sigalas *et al.* [8] have studied the important question of the effect of disorder on the transmittance of a PBG crystal. They used the transfer matrix method [9], which is a special case of a finite-difference method, to study the effects of disorder on the transmittance of two-dimensional photonic crystals composed of circular cylinders. They induced randomness by disordering the position, radius, or refractive index of the cylinders and observed the resulting appearance of states in the gap analogous to impurity states in semiconductors. Because of computer time constraints, their resolution of the states induced in the gap was low.

Another important question that is closely related to disordered photonic crystals is the question of the Anderson localization of electromagnetic waves [10]. Localization properties of electromagnetic waves in two-dimensional problems were studied numerically by de Raedt *et al.* [11], who considered the transverse localization of light. McGurn *et al.* [12] numerically studied the localization of electromagnetic waves emitted from a line source in a medium with a transverse randomness. In their investigations the authors [8,11,12] used a finite-difference method to study the localization of electromagnetic waves. Therefore, they were not able to give an analytical description of localization.

Recently we developed an accurate and highly efficient method for calculation of the transmittance properties of disordered photonic crystals [13] composed of circular cylinders. The method is based on a generalization of the Rayleigh method [14]. The photonic crystal under consideration is a stack of N_L gratings composed of circular cylinders as in Fig. 1. We have generalized the Rayleigh method to incorporate many cylinders per unit cell of the grating. Numerical efficiency and accuracy in calculating even very small transmittances are achieved by applying an inductive treatment [15], in which the reflection and the transmission coefficients of a stack are found recursively by using the reflection and transmission coefficients of single layers. This aspect of our treatment is similar to that employed by others [16–18].

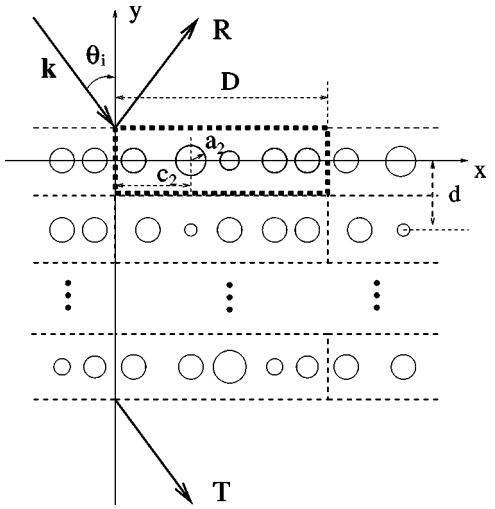

FIG. 1. The geometry of the problem. A plane wave of wave vector **k** is incident at an angle θ_i on a stack of gratings composed of N_c circular cylinders per unit cell (indicated by the heavy dashes), of radii a_i and centers c_i. The period of the grating is D and the separation of the layers is d, which is also the mean cylinder separation. Reflected and transmitted waves are labeled R and T, respectively.

The purpose of this article is twofold. First we investigate the effects of randomness on the transmittance of two-dimensional photonic crystals and study their homogenization properties in the long wavelength limit. Homogenization occurs when a photonic crystal can be viewed as a homogeneous medium with an effective dielectric constant, thus giving it the same optical properties as the actual medium [19,20]. If the wavelength is sufficiently large the wave does not distinguish the inhomogeneities in the stack and one can replace the stack of gratings with an equivalent medium of constant refractive index. Second we investigate the localization of electromagnetic waves in disordered two-dimensional lattices. In contrast to the finite-difference method, our method allows us not only to calculate numerically the properties of the random photonic crystals with high resolution, but also to give an analytical description of localization and homogenization.

The structure of this paper is as follows. In Sec. II we give a brief outline of our method. In Sec. III we study the effects of disorder on a photonic crystal in which the refractive index of the cylinders is randomized and consider the effects of disorder on the transmittance. We show that the behavior of the transmittance of the disordered photonic crystal is similar to that of the absorption of amorphous semiconductors. In Sec. IV we study homogenization and localization analytically and numerically. In all cases we find excellent agreement between theory and numerical simulations.

II. FORMULATION OF THE PROBLEM

Below we give a brief outline of our method in the scope required for subsequent applications in Sec. IV. The description of the method itself was reported in more detail in [13].

We consider a plane wave of wavelength λ incident in free space at an angle θ_i on the structure shown in Fig. 1. Each layer of this structure is a periodic grating that has a unit cell of length D, comprising a set of N_c nonoverlapping cylinders. The refractive indices of the cylinders are n_l, with radii a_l, all of which can be different. The centers of the cylinders are located on the same line and have the x coordinates c_l. Note that this restriction could be lifted and the positions of the centers of the cylinders could be arbitrary inside the unit cell, but we do not treat this case here. The stack consists of N_L such gratings of thickness h in the y direction, all of which are different. Thus the structure under consideration has $N_c N_L$ cylinders, which are periodically replicated in the x direction. The only essential requirement is that all layers must have the same period D. In the case of incidence perpendicular to the gratings [the two-dimensional (2D) case; see Fig. 1] the polarizations of waves are decoupled and the problem can be specified by a single component (H transverse to the generators of the grating) $V=E_z$ in the case of TM polarization and $V=H_z$ for TE polarization.

The solution of this problem is found in two steps. First, we find the reflection R and transmission T matrices of a single grating. Then by using an inductive treatment [15] we find the transmittance of the entire stack of gratings.

The essence of our approach to diffraction by a single grating is to exploit fully the geometry of the cylinders in determining the basis of functions to use. Cylindrical symmetry suggests that the wave field in the vicinity of the lth cylinder in the unit cell of a grating can be written in the Bessel expansion form

$$V(r_l,\theta_l)=\sum_{m=-\infty}^{\infty}[A_m^l J_m(kr_l)+B_m^l Y_m(kr_l)]e^{im\theta_l}, \quad (1)$$

for $r_l>a_l$, with a similar expansion for $r_l<a_l$. These expansions are matched at $r_l=a_l$ using the continuity of tangential components of electric and magnetic fields, which results in equations from which the A_m^l and internal ($r_l<a_l$) coefficients can be eliminated, giving [21]

$$A_m^l=-M_m^l B_m^l, \quad (2)$$

where

$$M_m^l=\frac{Z_l J_m'(n_l k a_l)Y_m(ka_l)-J_m(n_l k a_l)Y_m'(ka_l)}{Z_l J_m'(n_l k a_l)J_m(ka_l)-J_m(n_l k a_l)J_m'(ka_l)}. \quad (3)$$

Here $Z_l=n_l$ for E_z polarization and $Z_l=1/n_l$ for H_z polarization. The coefficients M_m^l determine the boundary condition matrix. It is seen that the boundary conditions are satisfied exactly through (3). This is significant advantage of this method, which allows use of measured refractive indices n_l of real materials [22]. Thus, the method can equally well be applied to dispersive, dissipative cylinders or cylinders with gain. Note that the contrast between the refractive index of the background and cylinders can be arbitrarily large.

The coefficients B_m^l are found using the Rayleigh identity, which is given by the relation [13]

$$\sum_{m=-\infty}^{\infty}S_{n-m}B_m^l+iM_n^l B_n^l+\sum_{q=1,q\neq l}^{N_c}\sum_{m=-\infty}^{\infty}S_{n-m}^{l,q}B_m^l = -i(-1)^n\exp[i(kc_l\sin\theta_i+n\theta_i)], \quad (4)$$

with

$$S_m=\sum_{n\neq 0}H_m^{(1)}(|n|kD)\exp(im\varphi_n)\exp(i\alpha_0 nD), \quad (5)$$

$$S_m^{l,q}=\sum_{n=-\infty}^{\infty}H_m^{(1)}(k|c_q-c_l+nD|)\exp(im\varphi_n)\exp(i\alpha_0 nD), \quad (6)$$

$$\alpha_p=k\sin\theta_p=k\sin\theta_i+2\pi p/D, \quad (7)$$

$$\chi_p=\begin{cases}\sqrt{k^2-\alpha_p^2}, & \alpha_p^2<k^2,\\ i\sqrt{\alpha_p^2-k^2}, & \alpha_p^2>k^2.\end{cases} \quad (8)$$

Here Eq. (7) determines the angle of propagating orders θ_p, where p is an integer and $\varphi_n=\pi H(-n)$, and $\varphi_0=\pi H(c_q-c_l)$ with H denoting the Heaviside function and $H_m^{(1)}$ is the Hankel function. Twersky [23] developed convenient expressions for accurate evaluation of the global lattice sums S_m, which are faster and more accurate than the widely used Ewald summation method [24].

The sums $S_m^{l,q}$ are local lattice sums, which depend on the cylinder l being treated as the local origin of coordinates, and the cylinder $q\neq l$ being considered as emitting waves to-

wards l. They can be obtained from global lattice sums using Graf's addition theorem [13]. The reflection and transmission coefficients R_p and T_p for order p of the grating can be written in the form [13]

$$R_p = \frac{2}{iD\chi_p} \sum_{m=-\infty}^{\infty} \sum_{l=1}^{N_c} B_m^l e^{-i(m\theta_p + \alpha_p c_l)}, \tag{9}$$

$$T_p = \delta_{p0} + \frac{2}{iD\chi_p} \sum_{m=-\infty}^{\infty} (-1)^m e^{im\theta_p} \sum_{l=1}^{N_c} B_m^l e^{-i\alpha_p c_l}, \tag{10}$$

with p being the order of diffraction (7), some of which can be evanescent.

The reflection $\mathcal{R}$ and transmission $\mathcal{T}$ matrices of the grating are also expressed in terms of the B_m^l coefficients. In the long wavelength limit we have only one propagating order (7) with $p=0$ and an infinite set of evanescent orders.

Using the recurrence approach developed previously [15], we calculate the reflection and the transmission of the entire stack of gratings. In numerical work, the accuracy of the method is determined by the number of modes $N_M = 2M+1$ and plane-wave coefficients $N_P = 2P+1$ retained, assuming the respective ranges are truncated to $-M \leqslant m \leqslant M$ and $-P \leqslant p \leqslant P$; by retaining sufficient numbers of modal coefficients and plane waves one can achieve any given accuracy. Illustrations of the accuracy of the method are given in [13]. All numerical results presented here have N_M and N_P chosen to yield five or more figures of precision.

III. DISORDERED TWO-DIMENSIONAL PHOTONIC CRYSTALS. NUMERICAL RESULTS

One of the important questions in designing photonic band-gap materials is the ability to predict the effects of disorder or imperfections on the transmittance properties of such materials [8]. In our system this disorder can be introduced by means of randomization of either the positions, radii, or refractive indices of the cylinders. Before disordering all these parameters at once it is important to know the effects of each type of disorder separately. In this paper we consider the effects of disorder induced by randomization of only the refractive indices of the cylinders. Thus for cylinder l we set

$$n_l = \overline{n} + \delta_l . \tag{11}$$

Here $\overline{n}$ is the regular part of the refractive index of the cylinders, while δ is a random variable uniformly distributed in the range $[-Q, Q]$. The disorder given by (11) is somewhat special because we retain the regular geometry of the lattice as in a random substitution alloy in the analogous electronic case. As we will see, this has a distinctive effect on the transmittance properties of the disordered PBG crystal. We distinguish two different cases: the *strong interface* case, in which the average cylinder refractive index is substantially different from that of the background (see Sec. III A) and the *weak interface* case, in which the average refractive index of the cylinders is equal to that of the background (see Sec. III B).

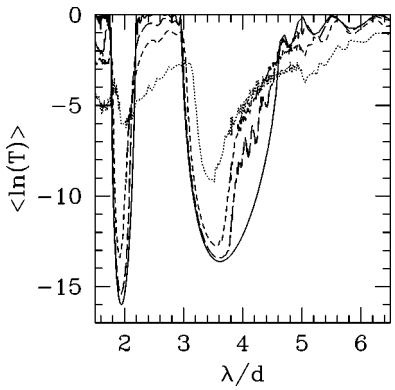

FIG. 2. Plot of $\langle \ln T \rangle$ vs wavelength for E_z polarization for $Q=0$ (solid), $Q=0.2$ (dashed), $Q=0.4$ (short dashed), $Q=0.8$ (dotted) for the strong interface case. Other parameters are given in the text.

In all numerical simulations the period of the unit cell is taken to be $D=5$ and there are $N_c=5$ cylinders in the unit cell, which are equally spaced by $d=D/5=1$. Note that the cylinders are considered dispersionless, and thus the unit of length is arbitrary: our results can be applied in any wavelength region in which materials with the relevant refractive index exist. There are $N_L=10$ layers in the stack with the same thickness d. The radii of the cylinders are all equal, with $a_l=0.3d$. We mainly consider the case of normal incidence ($\theta_i=0°$) of a plane wave (see Fig. 1) though some calculations for the case of off-axis incidence are also presented. The range of the random part of the refractive index δ is chosen to be $Q=0.2,0.4,0.6$, or 0.8.

By disordering the refractive indices n_l of the cylinders we investigate the changes in the structure of the bands. Mean properties are derived by averaging the logarithm of the transmittance over 100 realizations of the stack. For some wavelengths we carried out averaging over 400 realizations and the transmittance obtained was indistinguishable from the case of 100 realizations on the scale used in the figures. However, we found that a reduction to 25 realizations led to discernable differences.

A. Strong interface case

In the strong interface case, the regular part of the refractive indices of the cylinders is given by (11), with $\overline{n}=3$ in our calculations. The refractive index $\overline{n}=3$ is sufficient to develop strong band gaps.

In Fig. 2 we present results for $\langle \ln T \rangle$ as a function of wavelength for disorder, with $Q=0,0.2,0.4,0.8$ in the case of E_z polarization. The solid line represents the case $Q=0$ in which we do not have disorder. In this case, the structure develops two band gaps for wavelengths greater than $1.5d$. The first gap (counting from the right) is at wavelengths $\lambda \approx 3d-5d$ and the second gap is at $\lambda \approx 1.9d-2.1d$. Additional calculations (not shown) demonstrate that as we increase the refractive indices of the cylinders the gaps shift to longer wavelengths, while they deepen as we increase the number of layers. In the band gaps, the density of states, which is the number of propagating modes per unit frequency, vanishes in the limit of an infinite medium. By disordering the photonic crystal we induce impurity states in the

gap. This is similar to the case of the impurity states in doped semiconductors in the gap between the valence and conduction bands.

It is seen that the randomness $Q=0.2$ (dashed line in Fig. 2) affects $\langle \ln T \rangle$ compared with that of the regular structure ($Q=0$, solid line) more in the first gap than the second (see Fig. 2). We can see that the part of the first gap between $\lambda \approx 3.8d$ and $\lambda \approx 4.7d$ has been strongly affected by the disorder, with the transmission being greatly increased. The effects of disorder can also be seen to be very different on the short wavelength side of the first gap $3.0d<\lambda<3.8d$ from that of the long wavelength side. The second gap is affected in a way that the gap becomes slightly narrower. For the wavelengths outside the band gaps the randomness $Q=0.2$ reduces the transmittance of the regular structure between the gaps. For wavelengths greater than $\lambda \approx 5d$, $\langle \ln T \rangle$ is affected slightly if $Q=0.2$ because such long wavelengths cannot resolve the short-scale randomness.

As we increase the disorder to $Q=0.4$, $\langle \ln T \rangle$ is affected more by the disorder and both band gaps become shallower and narrower. In the regions $1.5d \leqslant \lambda \leqslant 1.75d$ and between the gaps ($2.2d \leqslant \lambda \leqslant 2.9d$) $\langle \ln T \rangle$ is reduced relative to the regular case. This reduction also takes place at longer wavelengths $4.7d<\lambda<5.2d$, while for wavelengths greater than $\lambda>5.2d$ the effects of randomness are small. Randomness with $Q=0.8$ has strong effects on the second gap, in which the transmittance substantially increases compared with the case of $Q=0.2$. The first gap becomes shallower and its long wavelength part at $3.7d<\lambda<4.7d$ is more strongly affected than the shorter wavelength part at $3d<\lambda<3.5d$.

We can understand the behavior of states near the gap edges by exploiting a direct analogy that exists between the wave equation in a periodic dielectric medium and the Schrödinger equation in a periodic lattice [3]. Specifically, the refractive index plays the role directly analogous to the potential energy in the electronic case, with high n_l corresponding to low potential [3]. In the electronic case, the appearance of a band gap implies the coexistence of two states at opposite sides of the gap with the same spatial periodicity as the lattice, one whose wave function is concentrated in atomic potential wells (regions of high n_l in the cylinders in the photonic analog), and the other in regions of higher potential (between the cylinders in the photonic case) [25]. The states concentrated in regions of low potential appear on the low-energy side of the gap, corresponding to the long-wavelength edge in the photonic analog.

When randomness (e.g., in the form of impurities) is introduced into a perfect semiconductor lattice, impurity states appear just inside the bandgap [25]. These states are spatially localized on the impurities. In the photonic case, the behavior seen in Fig. 2 is consistent with this picture: randomness in the cylinders' refractive indices gives rise to states inside the long-wavelength edge of the gap, whereas the short-wavelength edge is less affected because there is no randomness in the background medium in which these states are concentrated. We have also checked this interpretation by computing the transmittance for a stack where the mean refractive index of the cylinders was randomly chosen, but with an average smaller than unity. In this case, the short wavelength side of the gap was most affected by randomness, in accord with our theoretical picture.

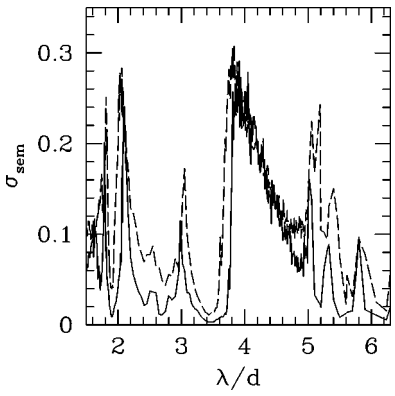

FIG. 3. Standard error of the mean [Eq. (12)] of $\langle \ln T \rangle$ vs wavelength for E_z polarization with $Q=0.2$ (solid) and $Q=0.4$ (dashed). Other parameters are given in the text.

We can see the approximately linear behavior of $\langle \ln T \rangle$ at the wavelengths $3.6d \leqslant \lambda \leqslant 3.8d$ and $3.9d \leqslant \lambda \leqslant 4.8d$ near the long-wavelength edge of the band gap (see Fig. 2). This behavior is reminiscent of the absorption spectrum of disordered semiconductors, which exhibit Urbach [26] and Tauc [27] tails near the band edges.

One of the characteristics of a random variable is the standard error of the mean σ_{sem}, which characterizes the uncertainty of a quantity averaged over N_r realizations; it is given by

$$\sigma_{\mathrm{sem}}=\frac{\sigma}{\sqrt{N_r}}, \tag{12}$$

where σ is the standard deviation of the individual measurements. In Fig. 3 we plot σ_{sem} for $\langle \ln T \rangle$. The standard error of the mean σ_{sem} is greater for randomness $Q=0.4$ than for $Q=0.2$ as expected. We can see that σ_{sem} has peaks at the wavelengths $\lambda \approx 2.9d$ and $\lambda \approx 3.9d$ which correspond to the positions of the edges of the first gap in Fig. 2, while the peaks at $\lambda \approx 1.8d$ and $\lambda \approx 2.1d$ of σ_{sem} correspond to the positions of the edges of the second gaps in Fig. 2.

The largest values of σ_{sem} seen in Fig. 3 occur around $\lambda \approx 4d$. At this wavelength the impurity states are localized on relatively short scales, and are thus much more affected by local randomness than longer-scale states at other wavelengths. The fact that the largest values of σ_{sem} occur toward the long-wavelength sides of the two gaps is also consistent with this picture, and with the electronic analog discussed earlier, since these states are concentrated in the cylinders where the randomness in the refractive index occurs. Correspondingly, in systems where the mean cylinder refractive index is less than that of the background, we find that σ_{sem} is largest on the short wavelength side of the gap.

In Fig. 4 we represent results for $\langle \ln T \rangle$ as a function of wavelength for disorder $Q=0.2$ and different angles of incidence $\theta_i=0°,30°,45°$. We see that at normal incidence the right edge of the gap is affected more by the randomness compared with the left edge of the gap; note that for all angles, the short wavelength side of the gap is smooth, while the long wavelength side has sharp features. This behavior is similar to the case of normal incidence. As we increase the

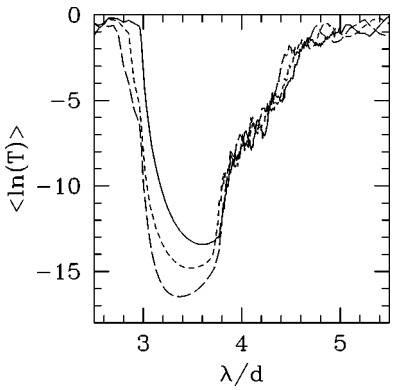

FIG. 4. Plot of $\langle \ln T \rangle$ vs wavelength for E_z polarization for $\theta_i = 0°$ (solid), $\theta_i = 30°$ (short dashed), $\theta_i = 45°$ (dashed). The disorder parameter for all figures is $Q = 0.2$. Other parameters are given in the text.

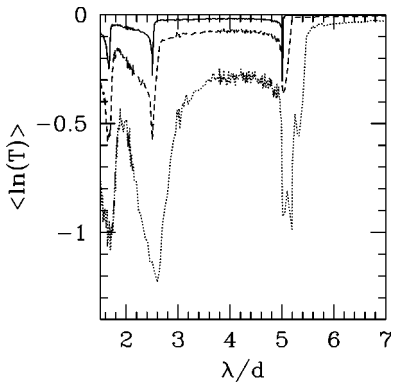

FIG. 6. Dependence of $\langle \ln T \rangle$ on wavelength for the case of E_z polarization for $Q = 0.2$ (solid), $Q = 0.4$ (dashed), and $Q = 0.8$ (dotted) for a weak interface case. Other parameters are given in the text.

incident angle θ_i from normal incidence, the center of the gap shifts towards shorter wavelengths and the gap deepens.

Figure 5 is similar to Fig. 2 but for H_z polarization. The solid line represents the case of an ordered photonic crystal with $Q = 0$. The structure develops two band gaps for wavelengths greater than $1.3d$. The first gap, which is at wavelengths $\lambda \approx 2.7d - 3d$, is very weak, while the second gap is at $\lambda \approx 1.4d - 2.2d$. As we can see, the second gap for H_z polarization is stronger than for the case of E_z polarization. The second gap consists of two parts separated by a narrow band at $\lambda \approx 1.62d$. The number of layers $N_L = 10$ is not sufficient to develop fully the first gap for H_z polarization. As we increase the number of layers from $N_L = 10$ to $N_L = 40,80$ we observe the development of this gap.

The randomness $Q = 0.2$ has a small effect on this weak gap at $\lambda \approx 2.8d - 3.1d$ (see Fig. 5). But as we increase the randomness to $Q = 0.6$ this gap almost vanishes. It is seen that the randomness has strong effects on the transmittance properties in the second gap for H_z polarization. As one expects, the narrow feature at $\lambda \approx 1.62d$ is rapidly destroyed by randomness. As the amount of randomness Q increases, the second gap becomes shallower. Similarly to the case of E_z polarization, we observe features reminiscent of Urbach and Tauc tails.

The above results demonstrate that disordered photonic crystals have similarities to disordered solids. The randomness affects the transmittance of H_z-polarized waves more than for the case of E_z polarization. For both polarizations we observe the appearance of states in the gap.

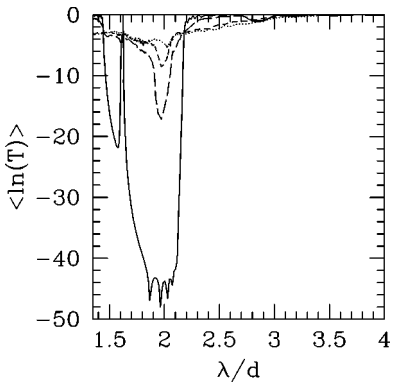

FIG. 5. Similar to Fig. 2, but for H_z polarization. Here $Q = 0$ (solid), 0.2 (dashed), 0.6 (dotted), and 0.8 (dot-dashed). Other parameters are given in the text.

B. Weak interface case

In this section we consider the effects of disorder for the weak interface case, in which the refractive index of cylinders is given by the relation $n_l = 1 + \delta$. In this case, when $Q = 0$, the refractive index of the cylinders is equal to the refractive index of the background and the medium is thus uniform. In Fig. 6 we present the dependence of $\langle \ln T \rangle$ on wavelength in the case of E_z polarization for $Q \neq 0$. It is seen that gaps develop in the vicinity of Wood anomalies $\lambda = D/p = 5,5/2,5/3 \ldots$, where $|p| = 1,2,3, \ldots$, [28]. At these wavelengths $|\alpha_p| = k$ and two of the diffraction orders (7) of the layer become parallel to the surface of the grating. Wood anomalies have long been known to be spectral regions in which grating properties are very sensitive to modifications of any structural characteristics. In the context of studies of photonic crystals, they correspond to light lines, which are defined by the dispersion equations of diffracted orders [see (7) and (8)]. The gaps being opened up correspond to the intersection points of two light lines.

As the amount of randomness increases the gaps increase in depth. Though these gaps are weak compared to the strong interface case (see Sec. III A), by adding more layers in the stack it is possible to make them stronger. In a way we can say that we can design random photonic crystals which have the average refractive constant equal to the refractive constant of the background but which develop gaps at wavelengths corresponding to the Wood anomalies $\lambda = D/|p|$ (see previous paragraph).

Figure 7 is similar to Fig. 6, but is for H_z polarization. In this case the disordered photonic crystal does not develop gaps in the vicinity of Wood anomalies, in contrast to the case of E_z polarization (Fig. 6). For $Q = 0.2$ (solid line), $\langle \ln T \rangle$ slightly increases with wavelength. As we increase the randomness to $Q = 0.4$ (dashed line) and 0.8 (dotted line), $\langle \ln T \rangle$ also decreases. This reduction is greater for shorter wavelengths than for long wavelengths.

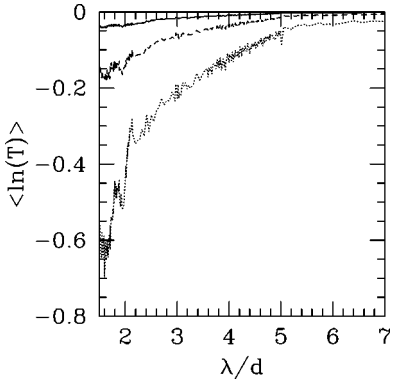

FIG. 7. Same as Fig. 6, but for H_z polarization.

IV. LONG-WAVELENGTH LIMIT

In the long-wavelength limit in which we have only one propagating order, the scattering matrices become scalars and it is possible to calculate analytically the transmittance and reflectance of the photonic crystal and find the effective refractive indices. In Sec. IV A we derive the effective dielectric constant of the photonic crystal for both polarizations for the case of normal incidence and we investigate the localization behavior of waves in this long wavelength regime in Sec. IV B.

A. Homogenization of a disordered photonic crystal

In the long-wavelength limit we show that each layer homogenizes and that the stack of layers thus homogenizes to a single slab with the appropriate effective dielectric constant, and thickness $N_L d$ (i.e., the total thickness of the stack). The homogenization takes place because at such long wavelengths the wave cannot resolve the structure of the photonic crystal. Here we derive the effective dielectric constant of the structure in Fig. 1.

First, we consider the case of E_z polarization. In the limit of long wavelengths it is sufficient to truncate the Rayleigh identity (4) and to keep only the modal coefficients of zeroth order B_0^l (monopole approximation)—see Sec. II. In this limit we have only one propagating order.

When λ is sufficiently large, $ka_l \ll 1$, and we expand the Bessel functions in the boundary condition coefficients M_m^l (3) in Taylor series and obtain [21]

$$M_0^l \approx \frac{4}{f\alpha^2(\varepsilon_l - 1)}, \tag{13}$$

$$M_1^l \approx \frac{32\pi}{f^2\alpha^4(\varepsilon_l - 1)}, \tag{14}$$

where $f = \pi a^2/d^2$ is the filling fraction, $\varepsilon_l = n_l^2$, and $\alpha = kd$. The long wavelength asymptotics for global lattice sums are given by [23]

$$S_0 \approx \frac{2}{kD}, \tag{15}$$

$$S_2 \approx -\frac{4\pi i}{3k^2D^2}. \tag{16}$$

In the case of normal incidence all global lattice sums of odd order $S_{2n-1} = 0$ vanish. The local lattice sums can be approximated as

$$S_0^{l,q} \approx \frac{2}{\alpha D}. \tag{17}$$

In this approximation we obtain $B_0^l \approx -1/M_0^l$. After substitution of this expression into (10) we find the reflection coefficient of zeroth order R_0 of the layer to be

$$R_0 \approx \frac{i\alpha}{2}\frac{1}{N_c}\sum_{l=1}^{N_c} f_l(\varepsilon_l - 1). \tag{18}$$

Quite generally, the equation of reflection coefficient of a single layer with a dielectric constant ε_{eff} and thickness d in the long-wavelength limit can be approximated as [15]

$$r_0 \approx \frac{i\alpha}{2}(\varepsilon_{\text{eff}} - 1). \tag{19}$$

By comparing equations (18) and (19) we find that the effective dielectric constant for the grating is

$$\varepsilon_{\text{eff}} = 1 + \frac{1}{N_c}\sum_{l=1}^{N_c} f_l(\varepsilon_l - 1). \tag{20}$$

The effective dielectric constant of the random layer can be found by averaging (20)

$$\langle \varepsilon_{\text{eff}} \rangle = 1 + \frac{1}{N_c}\left\langle \sum_{l=1}^{N_c} f_l(\varepsilon_l - 1) \right\rangle. \tag{21}$$

where $\langle \cdots \rangle$ denotes ensemble averaging. If f_l and ε_l are uncorrelated, the effective dielectric constant of the random layer can be found by averaging (20), which gives

$$\langle \varepsilon_{\text{eff}} \rangle = 1 + f\left(\overline{n^2} + \frac{Q^2}{3} - 1 \right), \tag{22}$$

where f is the average of the filling fraction $f = \langle f_l \rangle$. If each layer is statistically equivalent, each grating in the stack homogenizes to the same value of the effective dielectric constant (20). Therefore the stack of layers also homogenizes to this value.

In Fig. 8 we plot on a logarithmic scale the inverse of the average of the logarithm of the transmittance with the parameters as in Sec. III A for randomness $Q = 0.2$. The same quantity is calculated for a slab of a dielectric with the effective dielectric constant $\langle \varepsilon_{\text{eff}} \rangle$ from (22). Excellent agreement between two curves is seen even for wavelengths as low as $\lambda \approx 5d$. The resonances in the range $5d < \lambda < 40d$ are Fabry-Perot effects. This plot implies that the random set of dielectric cylinders homogenizes to a dielectric slab with effective dielectric constant ε_{eff} given by the relation (22).

Now we consider the case of the H_z polarization. In analogy to (13) and (14) we find [21]

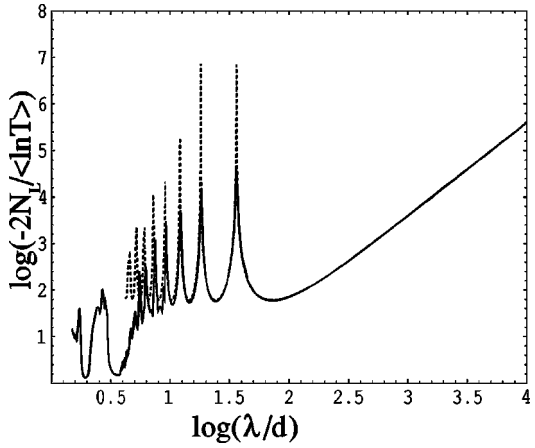

FIG. 8. Dependence of $-2N_L/\langle \ln T\rangle$ on λ for E_z polarization (solid line) and $Q=0.2$. The dashed line represents the inverse of the transmittance of a slab with effective dielectric constant ε_{eff} from Eq. (22) and thickness $N_L d$.

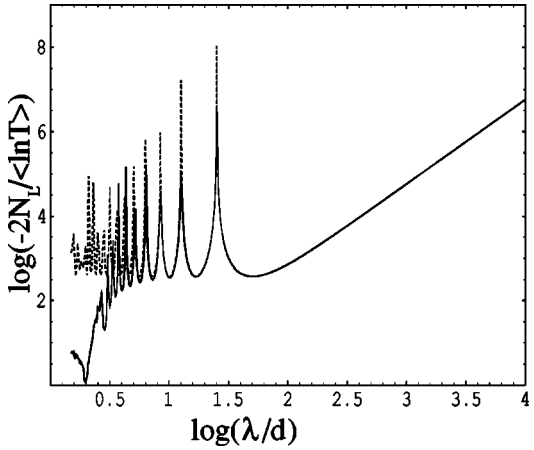

FIG. 9. Same as Fig. 8, but for H_z polarization. The dashed line represents the inverse of the transmittance of a slab with effective dielectric constant ε_{eff} from Eq. (31) and thickness $N_L d$.

$$M_0^l \approx \frac{32\pi}{f_l^2 \alpha^4 (\varepsilon_l - 1)}, \tag{23}$$

$$M_1^l \approx \frac{4}{f_l \alpha^2} \frac{\varepsilon_l + 1}{\varepsilon_l - 1}. \tag{24}$$

However, now the dipole approximation is required as the dipole coefficients $B_{\pm 1}^l$ are larger than the monopole coefficients B_0^l for each cylinder. In the case of weak randomness $\delta_l \ll \overline{n}$ the solution of the Rayleigh identity (4) can be approximated as

$$B_{-1}^l \approx B_1^l \approx \frac{i}{S_2 + iM_1^l + \sum_{q=1, q\neq l}^{N_c} S_2^{l,q}}, \tag{25}$$

$$B_0^l \approx O(\alpha^3). \tag{26}$$

By taking into account the relation

$$\sum_{q=1, q\neq l}^{N_c} S_2^{l,q} \approx (N_c^2 - 1) S_2, \tag{27}$$

derived in the Appendix, the reflection of a single layer can be written in the form

$$R_0 = -\frac{i\alpha}{2} \frac{1}{N_c} \sum_{l=1}^{N_c} \frac{2 f_l}{\frac{\varepsilon_l + 1}{\varepsilon_l - 1} - \frac{\pi}{3} f_l}. \tag{28}$$

From (28), and in a similar manner as for E_z polarization, the effective dielectric constant can be written in the form

$$\varepsilon_{\text{eff}} = 1 + \frac{1}{N_c} \sum_{l=1}^{N_c} \frac{2 f_l}{\frac{\varepsilon_l + 1}{\varepsilon_l - 1} - \frac{\pi}{3} f_l}, \tag{29}$$

which is valid for the case of weak randomness $\delta_l \ll \overline{n}$. The effective dielectric constant of the random layer can be found by averaging (29) over the refractive index distribution. If the filling fractions f_l are the same for all cylinders, and exploiting the weakness of randomness, $\langle \varepsilon_{\text{eff}} \rangle$ takes the form

$$\langle \varepsilon_{\text{eff}} \rangle = 1 + \frac{2f}{\frac{\overline{n^2} + 1}{\overline{n^2} - 1} - \frac{\pi}{3} f} - \frac{4Q^2 f \left[3\overline{n^2} - 1 - \frac{\pi f}{3} (3\overline{n^2} + 1) \right]}{3 \left[\overline{n^2} + 1 - \frac{\pi f}{3} (\overline{n^2} - 1) \right]^3}. \tag{30}$$

In the case when randomness $Q=0$ we deduce from (30)

$$\langle \varepsilon_{\text{eff}} \rangle = 1 + \frac{2f}{\frac{\overline{n^2} + 1}{\overline{n^2} - 1} - \frac{S_2}{\pi} f}. \tag{31}$$

Here, $S_2/\pi = \pi/3$ for a single layer, and $S_2/\pi = 1$ for an infinite stack of layers. The latter case is the Maxwell Garnett formula [31]. The small difference between $\pi/3$ and unity occurs because, for H_z polarization, it is necessary to take into account evanescent couplings between the layers of the stack. In Fig. 9 we plot the inverse of $\langle \ln T \rangle$ versus wavelength for the same parameters as in Sec. III A for randomness $Q=0.2$ (solid line). The same quantity is also shown estimated for a slab of a dielectric with the effective dielectric constant ε_{eff} (30) (dashed line). Excellent agreement between the two results is again seen for wavelengths as small as $\lambda \approx D = 5d$.

For a small number of cylinders per unit cell one can solve the Rayleigh identity (4) using computer algebra and find the effective dielectric constant without the requirement of weak randomness. For example in the case of two cylinders per unit cell $N_c = 2$ the effective dielectric constant takes the form

$$\varepsilon_{\text{eff}}=1+\frac{\frac{1}{f_1}\frac{\varepsilon_1+1}{\varepsilon_1-1}+\frac{1}{f_2}\frac{\varepsilon_2+1}{\varepsilon_2-1}+\frac{\pi}{3}}{\left(\frac{1}{f_1}\frac{\varepsilon_1+1}{\varepsilon_1-1}-\frac{\pi}{12}\right)\left(\frac{1}{f_2}\frac{\varepsilon_2+1}{\varepsilon_2-1}-\frac{\pi}{12}\right)-\frac{\pi^2}{16}}, \tag{32}$$

where ε_i, and f_i are the dielectric constants and filling fractions of cylinders. Equation (32) is an extension of the Maxwell Garnett formula [31] for the effective dielectric constant of a composite material, when we have two inclusions inside the unit cell. If the cylinders have the same dielectric constant and filling fractions, (32) reduces to (31).

B. Crossover from localization to homogenization

Localization of electromagnetic waves can occur when waves undergo multiple scattering off a random potential. The destructive interference completely changes the character of the wave transport from free propagation to diffusive propagation and, as scattering increases further, the constant of diffusion tends to zero, localization sets in and photon transport stops completely. One of the characteristics of localization is the localization length l^* which is defined by the relation [29]

$$\frac{l^*}{d}=-\lim_{N_L\to\infty}\frac{2N_L}{\langle \ln T\rangle}, \tag{33}$$

where T is the transmittance of the stack of N_L layers and d is the thickness of each layer. The localization length parameterizes the transmission properties of a random semi-infinite system and represents a length of attenuation. This is roughly the scale over which the constant of diffusion tends to zero due to complete destructive interference being established.

Usually, in numerical calculations a localization scaling length l is calculated using a finite value for N_L [30], with

$$\frac{l}{d}=-\frac{2N_L}{\langle \ln T\rangle}. \tag{34}$$

In the long-wavelength limit l incorporates Anderson localization and attenuation due to Fabry-Perot reflections between the first and the last interfaces of the slab (for more discussion see [15]). Thus the difference between l^* and l is that the latter takes into account the effects of the multiple reflections from the first and the last interfaces of the stack. For sufficiently long stacks l approaches l^*.

In [15] we obtained a general expression for the localization scaling length l of plane waves normally incident on a stack of N_L layers of thickness d and random complex dielectric constant ε_s. In the case of dielectric layers the localization scaling length in the long-wavelength limit can be written in the form

$$\frac{d}{l}=\frac{\alpha^2}{8}[\langle \eta^2\rangle+N_\alpha\overline{\varepsilon^2}]. \tag{35}$$

Here $\overline{\varepsilon}=\langle \varepsilon_s\rangle-1$, $\alpha=kd$ and η is the random component of the dielectric constant with zero average $\langle \eta\rangle=0$ and N_α is the switch term given by

$$N_\alpha=2+\frac{\sin(N_L\alpha)\sin[(N_L-2)\alpha]}{N_L\sin^2\alpha}. \tag{36}$$

The switch term converges rapidly to the number of layers in the stack $N_\alpha\to N_L$ as the wavelength increases ($\alpha\to 0$), while for the short wavelengths it is of order unity $N_\alpha\approx 1$. The first term in (35), which does not depend on the number of layers in the stack, determines the localization length l^*. The second term describes multiple reflections from the first and last interfaces of the stack.

We consider below the case of E_z polarization. Let the filling fractions f_l of the cylinders be same. After substitution of (11) into (20), ε_{eff} can be written in the form

$$\varepsilon_{\text{eff}}=1+\overline{\varepsilon}+\eta, \tag{37}$$

where $\overline{\varepsilon}$ and η are given by the relations (22)

$$\overline{\varepsilon}=f(\overline{n^2}-1)+\frac{fQ^2}{3}, \tag{38}$$

$$\eta=\frac{2f\overline{n}}{N_c}\sum_{l=1}^{N_c}\delta_l+\frac{f}{N_c}\sum_{l=1}^{N_c}\delta_l^2-\frac{fQ^2}{3}. \tag{39}$$

By averaging uniformly distributed random variables δ_l over the range $[-Q,Q]$ we obtain

$$\langle \eta^2\rangle=\frac{4f^2\overline{n^2}Q^2}{3N_c}+\frac{4f^2Q^4}{45N_c}. \tag{40}$$

After substitution of (40) into (35) and taking into account $\delta\ll 1$, the localization length for the weak interface case $\overline{n}=1$ for $\lambda>D$ takes the form

$$\frac{l^*}{d}=\frac{3N_c}{2\pi^2f^2Q^2}\left(\frac{\lambda}{d}\right)^2. \tag{41}$$

Equation (41) implies that the localization length l^* is proportional to the square of the wavelength, which is similar to the case of one-dimensional problems [30]. Another interesting feature of (41) is the proportionality of the localization length to the number of cylinders N_c per unit cell. This does not imply an unphysical divergence as N_c increases, because (41) is only valid for $\lambda>N_cd$; if N_c exceeds λ/d, multiple propagating orders must be incorporated and the above analysis breaks down.

After substitution of (40) and (39) into (35) the localization scaling length can be written in the form

$$\frac{l}{d}=\frac{3N_c}{2\pi^2f^2Q^2\left(1+\frac{N_cN_\alpha Q^2}{12}\right)}\left(\frac{\lambda}{d}\right)^2. \tag{42}$$

In Fig. 10 we plot the dependence of $(l/d)/(\lambda/d)^2$ on wavelength λ/d for the weak interface case for the same parameters as in Sec. III B and randomness $Q=0.4$. The solid line represents our numerical simulation of (34), the long dashed line is based upon Eq. (41), while the short-dashed line represents estimate (42), in which the switch

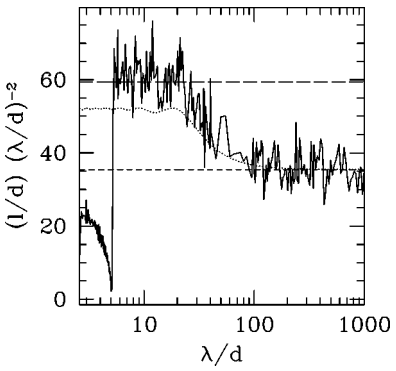

FIG. 10. Dependence of l on wavelength Eq. (34) (solid line) for E_z polarization and $Q=0.4$. The upper dashed line represents the localization length behavior l^* Eq. (41), while the lower dashed line is given by Eq. (42) in which we use the asymptotic value for $N_\alpha = N_L$. The dotted line represents the crossover from the localization to homogenization predicted by Eq. (42).

term is replaced by its asymptotic limit $N_\alpha = N_L$. The dotted line that describes the crossover from localization to homogenization is given by Eq. (42). It is seen that there is a crossover from localization to homogenization near $\lambda \approx 4N_L d$. At such long wavelengths the effects of scattering between the cylinders diminish and structure is effectively homogeneous.

V. CONCLUSION

We have studied the effects of disorder on two-dimensional photonic crystals composed of circular cylinders. As shown, the optical transmittance properties of disordered photonic crystals are reminiscent of the absorption spectra of amorphous semiconductors, particularly in that they exhibit tail-like features near the band edges.

In the limit of long wavelengths the structure homogenizes and we obtain the effective dielectric constants for disordered photonic crystals for both polarizations. In this region our numerical simulations and analytic calculations are in excellent agreement with each other.

In the *weak interface* case, in which the average refractive index of the cylinders is equal to that of the background, we studied the transmittance properties of such random photonic crystals for both polarizations. Such photonic crystals develop gaps at points where light lines intersect (i.e., double Rayleigh wavelengths) for the case of E_z polarization, while for the case of H_z polarization we did not observe the development of the band gaps at these wavelengths.

In the limit of long wavelengths we have obtained the localization length behavior as the function of wavelength. We have shown that the localization length is proportional to the square of the wavelength similarly to the case of one-dimensional stratified random layers. Interestingly, the localization length is also proportional to the number of cylinders N_c per unit cell. We have shown that for long wavelengths there is a crossover from localization to homogenization.

ACKNOWLEDGMENTS

Helpful discussions with B. L. Altshuler, D. R. McKenzie, and C. M. Soukoulis are acknowledged. The Australian Research Council supported this work.

APPENDIX: DERIVATION OF THE RELATION (27)

By applying Graf's addition theorem [32] the local lattice sum S_2^{lq} (7) for the case of normal incidence can be expressed in the form [13]

$$S_2^{lq} = iY_2(k|c_q - c_l|) + \sum_{n=-\infty}^{\infty} S_{2n+2} J_{2n}(k|c_q - c_l|). \tag{A1}$$

The long-wave asymptotic of the global lattice sums S_n are [23]

$$S_{2n} \approx \frac{i(-1)^n 2^{2n-1}(2\pi)^{2n} B_{2n}}{\pi n \alpha^{2n}}, \tag{A2}$$

where B_{2n} are Bernoulli numbers

$$B_{2n} = \frac{(-1)^{n-1} 2(2n)!}{(2\pi)^{2n}} \zeta(2n), \tag{A3}$$

$$\zeta(2n) = \sum_{s=1}^{\infty} \frac{1}{s^{2n}}. \tag{A4}$$

Here $\zeta(2n)$ is the Riemann's zeta function. The asymptotic values for $Y(k|c_q - c_l|)$ and $J_{2n}(k|c_q - c_l|)$ as $k \to 0$ are [32]

$$Y_2(k|c_q - c_l|) \approx -\frac{4}{\pi k^2 |c_q - c_l|^2}, \tag{A5}$$

$$J_n(k|c_q - c_l|) \approx \frac{k^n |c_q - c_l|^n}{2^n n!}. \tag{A6}$$

After substitution of (A6), (A5), and (A2) into (A1) S_2^{lq} takes the form

$$S_2^{lq} \approx -\frac{4i}{\pi k^2 |c_l - c_q|^2} - \frac{8i}{\pi k^2 |c_l - c_q|^2} \times \sum_{n=1}^{\infty} (2n-1) \frac{(c_l - c_q)^{2n}}{D^{2n}} \zeta(2n). \tag{A7}$$

The series in (A7) can be calculated in closed form. We substitute (A4) into (A7) and by changing the order of summation and using the relation

$$\sum_{s=1}^{\infty} (a + sr) q^s = \frac{aq}{1-q} + \frac{rq}{(1-q)^2}, \tag{A8}$$

(see [33], p. 7) (A7) can be written in the form

$$S_2^{lq} \approx -\frac{4i}{\pi k^2 |c_l - c_q|^2} - \frac{8i}{\pi k^2 |c_l - c_q|^2} \sum_{s=1}^{\infty} \frac{a^2 s^2 + a^4}{(s^2 - a^2)^2}, \tag{A9}$$

where a denotes

$$a = \frac{c_l - c_q}{D}. \tag{A10}$$

The series in (A9) can be calculated using the relations (see [34], p. 687, Eq. (25), Eq. (35)).

$$\sum_{s=1}^{\infty} \frac{1}{(s^2-a^2)^2} = -\frac{1}{2a^4} + \frac{\pi}{4a^3}\cot(\pi a) + \frac{\pi^2}{4a^2}\csc^2(\pi a), \tag{A11}$$

$$\sum_{s=1}^{\infty} \frac{s^2}{(s^2-a^2)^2} = -\frac{\pi}{4a}\cot(\pi a) + \frac{\pi^2}{4}\csc^2(\pi a). \tag{A12}$$

By using the relations (A11)–(A12), S_2^{lq} can be written as

$$S_2^{lq} \approx -\frac{4\pi i}{(kD)^2}\csc^2\left(\pi\frac{c_l-c_q}{D}\right). \tag{A13}$$

By taking into account Eqs. (16) and (A13) takes the form

$$S_2^{lq} \approx 3S_2\csc^2\left(\pi\frac{c_l-c_q}{D}\right). \tag{A14}$$

In the case in which the distance $d=D/N_c$ between the centers of the cylinders per unit cell is same we can write $c_q = c_l+(q-l)d$ and (A14) takes the form

$$S_2^{lq} \approx 3S_2\csc^2\left(\pi\frac{q-l}{N_c}\right). \tag{A15}$$

Without loss of generality we can set $l=1$ and (27) can then be obtained using the relation [see [34], p. 644, Eq. (5)]

$$\sum_{s=1}^{N-1} \csc^2\left(\frac{s\pi}{N}\right) = \frac{N^2-1}{3}. \tag{A16}$$

[1] E. Yablonovitch, Phys. Rev. Lett. **58**, 2059 (1987).

[2] *Photonic Band Gap Materials*, edited by C. M. Soukoulis, Vol. 315 of *NATO Advanced Study Institute Series B* (Kluwer, Dordrecht, 1995).

[3] J. D. Joanopoulos, R. D. Meade, and J. N. Winn, *Photonic Crystals: Molding the Flow of Light* (Princeton University Press, Princeton, NJ, 1995).

[4] J. Dowling, H. Everitt, and E. Yablonovitch, *Photonic and Acoustic Band-Gap Bibliography*, http://home.earthlink.net/jpdowling/pbgbib.html

[5] P. Tran, Opt. Lett. **21**, 1138 (1996).

[6] E. Yablonovitch, J. Opt. Soc. Am. B **10**, 283 (1993).

[7] E. R. Brown, C. D. Parker, and E. J. Yablonovitch, J. Opt. Soc. Am. B **10**, 404 (1993).

[8] M. M. Sigalas, C. M. Soukoulis, C.-T. Chan, and X. Turner, Phys. Rev. B **53**, 8340 (1996).

[9] J. B. Pendry and A. MacKinnon, Phys. Rev. Lett. **69**, 2772 (1992).

[10] S. John, Phys. Rev. Lett. **53**, 2169 (1984).

[11] H. De Raedt, Ad Lagendijk, and P. de Vries, Phys. Rev. Lett. **62**, 47 (1989).

[12] A. R. McGurn, P. Sheng, and A. A. Maradudin, Opt. Commun. **91**, 175 (1992).

[13] R. C. McPhedran, L. C. Botten, A. A. Asatryan, N. A. Nicorovici, P. A. Robinson, and C. M. de Sterke, Aust. J. Phys. **791** (1999).

[14] Lord Rayleigh, Philos. Mag. **34**, 481 (1892).

[15] L. C. Botten, C. M. de Sterke, R. C. McPhedran, N. A. Nicorovici, A. A. Asatryan, and P. A. Robinson (unpublished).

[16] N. Stefanou and A. Modinos, J. Phys.: Condens. Matter **3**, 8135 (1991).

[17] D. Maystre, Pure Appl. Opt. **3**, 975 (1994).

[18] P. Dansas and N. Paraire, J. Opt. Soc. Am. A **15**, 1586 (1998).

[19] Z. Hashin, J. Appl. Mech. **105**, 481 (1983).

[20] J. D. Jackson, *Classical Electrodynamics* (Wiley, New York, 1975).

[21] R. C. McPhedran, N. A. Nicorovici, and L. C. Botten, J. Electromagn. Waves Appl. **11**, 981 (1997).

[22] E. D. Palik, *The Handbook of Optical Constants of Solids* (Academic, New York, 1993).

[23] V. Twersky, Arch. Ration. Mech. Anal. **8**, 323 (1963).

[24] M. L. Glasser and I. J. Zucker, *Theoretical Chemistry: Advances and Perspectives* (Academic, New York, 1980), Vol. 5, p. 67.

[25] C. Kittel, *Solid State Physics* (Wiley, New York, 1986).

[26] F. Urbach, Phys. Rev. **92**, 1324 (1953).

[27] N. E. Cusack, *The Physics of Structurally Disordered Matter* (University of Sussex, Bristol, 1987).

[28] M. C. Hutley, *Diffraction Gratings* (Academic, New York, 1982).

[29] V. D. Freilikher and S. A. Gredeskul, Prog. Opt. **30**, 137 (1990).

[30] C. M. de Sterke and R. C. McPhedran, Phys. Rev. B **47**, 7780 (1993).

[31] J. C. Maxwell Garnett, Philos. Trans. R. Soc. London, Ser. A **203**, 385 (1904).

[32] *Handbook of Mathematical Functions* edited by M. Abramowitz and I. A. Stegun (Dover, New York, 1980).

[33] I. S. Gradshteyn and I. M. Ryzhik, *Table of Integrals, Series and Products*, 4th ed. (Academic, New York, 1980).

[34] A. P. Prudnikov, Yu. A. Brychkov, and O. I. Marichev, *Integrals and Series* (Gordon & Breach, New York, 1986), Vol. 1.